Key Engineering Materials
ISSN: 1662-9795, Vol. 963, pp 11-17
doi:10.4028/p-Extn3M

Submitted: 2023-05-26
Accepted: 2023-06-14
Online: 2023-10-13

The Liquid Fraction of ZA27 Zinc Alloy from TLP Diffusion Bonding Affecting Mechanical Properties and Microstructural Characterizations of SSC-ADC12 Aluminum Alloy

Chaiyoot Meengam[1,a,*], Yongyuth Dunyakul[2,b] and Dech Maunkhaw[3,c]

[1]Faculty of Industrial Technology, Songkhla Rajabhat University, Songkhla, Thailand

[2,3]Department of Industrial Engineering, Faculty of Engineering, Rajamangala University of Technology Srivijaya, Songkhla, Thailand

[a]Chaiyoot.me@skru.ac.th, [b]Dyongyuth@gmail.com, [c]Dechmaunkhaw@yahoo.com

Keywords: ZA27 Zinc Alloy; SSC-ADC12 Aluminum Alloy; Liquid Fraction; TLP Diffusion Bonding

Abstract. This work investigated liquid fraction in ZA27 zinc alloy interlayered with SSC-ADC12 aluminum alloy workpieces for Transient Liquid Phase (TLP) diffusion bonding. The results clearly indicated that liquid fraction had a necessary influence on TLP diffusion bonding. In other words, the high liquid fraction and bonding time tends to produce excellent bond strength. The maximum bond strength at 27.21 MPa was from 100% liquid fraction and 90 min from bonding time. The hardness increased by approximately 23.36% comparing to SSC-ADC12 aluminum alloy and by 11.18% comparing to the ZA27 zinc alloy. The microstructure was homogeneous in the bond line and formed to $MgZn_2$ and $CuZn_4$ intermetallic compound under Scanning Electron Microscope. According to Energy Dispersive X-Ray Spectrometer analysis, Zn atoms had the ability to move about 4.381 mm from the bond line and the elements' uniform distribution.

Introduction

Transient Liquid Phase (TLP) diffusion bonding is a method that was further developed from diffusion welding to solve the problem of difficult welding for metallic and ceramic materials. The unique characteristic feature of the TLP is selecting the right solder material which is the most important mechanism affecting adhesion and mechanical properties [1]. The solder material will melt momentarily and form a liquid state while the substrate materials remain solid status. In this step, the element diffuses into the substrate materials. Therefore, the atomic diffusion mechanism starts from the solder material to the substrate materials. When the diffusion time for atomic diffusion is adequate, this will lead to a completed workpiece [2]. However, the success of TLP diffusion bonding should considere which types of solder materials is recommended to have a chemical composition that is not too different from the substrate material. But the melting point of solder materials must have a lower temperature. Besides, the bonding time and the bonding temperature also play an essential role in this TLP diffusion bonding. In particular, the bonding temperature affects the amount of liquid fraction of solder formed during welding. Thereby, this could affect the formation of defects after welding [3] and is a foremost cause of bonded strength [4]. Likewise, the TLP diffusion bonding atmosphere is also necessary for welding. In other words, the typical weld atmosphere conditions result in moisture disturbances in the transient liquid phase [5], which could be a failure for TLP diffusion bonding. Therefore, the recommendations in a vacuum atmosphere for TLP diffusion bonding were explained [6-7]. In addition, gas atmosphere is another suggestion that many researchers previously studied [8-9].

The semi-solid cast (SSC) materials is a modern casting process against to solve crack, porosity, shrinkage, and defect problems from original casting [10]. The semi-solid casting method controls the casting temperature to the semi-solid range. Then, use mechanical techniques or the reaction to assist the microstructural changes forming the shape of a uniform globular grain [11]. SSC-ADC12 aluminum alloy is another material that is molded by semi-solid casting. It was produced to respond the needs of the automotive industry. Especially, SSC-ADC12 aluminum alloy is used to produce engine parts, door parts, and etc.,[12]. However, the study of welding of semi-solid materials is still in the great interest due to the changing shape of the microstructure from the base structure [13]. Consequently, in this study, liquid fraction of ZA27 zinc alloy with TLP diffusion bonding and SSC-ADC12 aluminum alloy rod exerting influence on bond strength, hardness and microstructural characterizations was investigated.

The liquid fraction of ZA27 zinc alloy is solder material during TLP diffusion bonding showing significant effects on the mechanical properties and microstructure transformation. Thereby, liquid fraction enabling changes in bonding temperature was therefore important in this study. The experiment results were evaluated and analysed to determine the suitable variables for TLP diffusion bonding.

Materials and Methods

Materials. The materials in the experiment were the wrought ZA27 zinc alloy in a rod shape with the dimensions of Ø12×0.3 mm^3. The tensile strength was at 417 MPa with 5% elongation, and Vicker hardness was at 107.20 HV with melting point at 399ºC respectively. The SSC-ADC12 aluminum alloy was formed by the GISSCO limited company from Thailand with Gas Induce Semi-Solid Metal technique developed by J.Wannasin et al [14]. The dimensions of SSC-ADC12 aluminum alloy was Ø12×60 mm^3 in rod shape as well. The tensile strength of SSC-ADC12 aluminum alloy was at 331 MPa with 3% elongation, and Vicker hardness was at 92.50 HV with melting point at 399ºC. The chemical composition of materials in the experiment are shown in Table 1.

Table 1. The chemical compositions of SSS-ADC12 Aluminum Alloy and ZA27 zinc alloy.

Materials	Si	Cu	Fe	Zn	Mn	Ni	Mg	Sn	Other	Al
SSC-ADC12	11.99	1.75	0.93	0.78	0.12	0.11	0.07	0.03	0.03	Bal.
ZA27	0.81	3.22	0.02	Bal.	0.82	0.05	0.91	-	-	4.20

Methods in Experiment. The liquid fraction is the amount of liquid of ZA27 zinc alloy. This experiment studied the range of liquid fraction between 60-100% was melting point when derived from the calculation according to the Lever rule [15]. The fraction will be amenable to the change in bonding temperature shown in Table 2. The liquid fraction plays an important role in the bond strength, distance of the atomic diffusion, eutectic transformation, and the formation of defects respectively.

Table 2. The percentage of liquid fraction of ZA27 zinc alloy was calculated.

Bonding Temperatures (oC)	Liquid Fraction (%)
239.4	60
279.3	70
319.2	80
359.1	90
399.0	100

For the TLP diffusion bonding method, the surface preparation of the workpiece has to be careful because the surface roughness significantly affects the atomic diffusion. Thereby, the surface roughness of ZA27 zinc alloy and SSC-ADC12 aluminum alloy were scrubbed with sandpaper No.1200. Then, the workpiece was steadily pressed at 2.9 MPa by centering the ZA27 zinc alloy between the SSC-ADC12 aluminum alloy. After that argon gas atmosphere was released into the furnace with the flow rate at 16 litres per minute, following by control bonding temperature according to the proportion of liquid fraction. For bonding time derived from previous experiments, when bonding time was set in the range of 45 to 90 minutes. The TLP diffusion bonding process of SSC-ADC12 aluminum alloy and ZA27 zinc alloy were interlayered shown in Fig. 1.

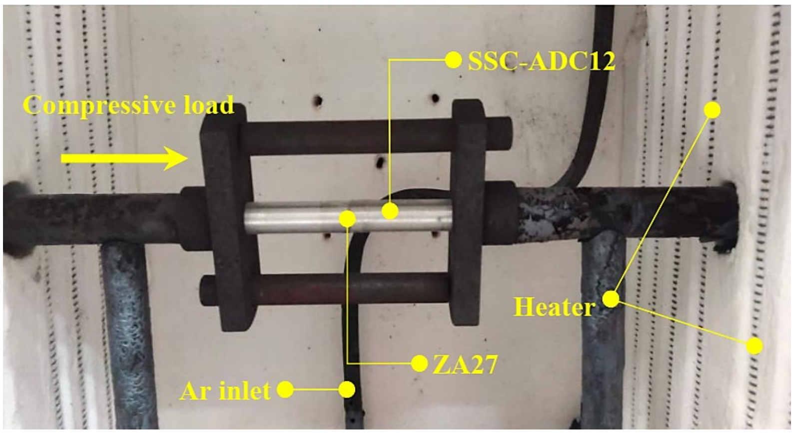

Figure 1. Schematic diagram TLP diffusion bonding of SSC-ADC12 aluminum alloy, when ZA27 zinc alloy was interlayer.

Results and Discussion

Characteristics of Workpiece After TLP Diffusion Bonding. The workpiece was perfect in all experimental conditions shown in Fig. 2 when bonding time at 45 min shown in Fig. 2 (a-e) and bonding time at 90 min shown in Fig. 2 (f-j), respectively. It is noticeable the different liquid fraction ratios influences deformation. Obviously, the 100% liquid fraction causes severe deformation due to heat dissipation from the transient liquid status. This indicates that the comparison of high liquid fraction clearly affects the buckling deformation, particularly in the bond line (Fig. 2(e and j)), and in the bond line in the joint of some variables. The expansion and swelling was observed (Fig. 2(g-i)). Coherently, the high liquid fraction and bonding time leads to heat distribution resulting in the broader diffused zone (Fig. 2(j)). However, some of the ZA27 zinc alloy were pushed out of the joint, which has a tubercle characteristic shown in (Fig. 2(b-e and g-i)). The plastic deformation of the workpiece after TLP diffusion bonding exerts influence on bond strength because buckling or expanding and swelling workpieces will have the ability to withstand the axis force has decreased [16].

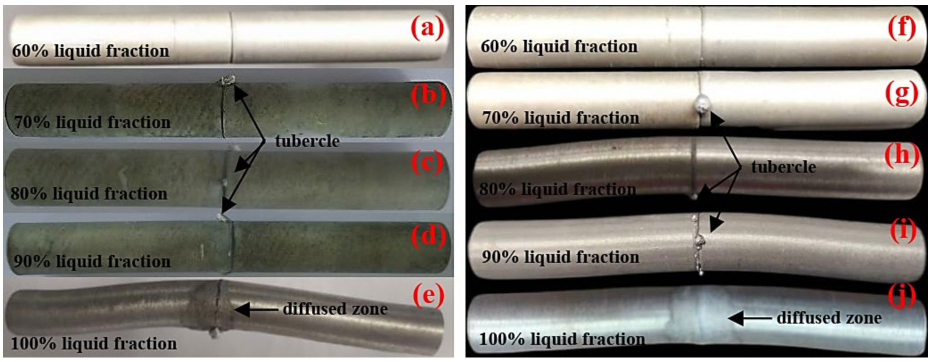

Figure 2. Characterizations of workpiece deformation from TLP diffusion bonding.

Bond Strength Comparison of Liquid fraction Analysis. The bond strength profiles of SSC-ADC12 aluminum alloy TLP diffusion bonding using ZA27 zinc alloy interlayer are shown the Fig. 3. This indicated that a maximum bond strength at 27.21 MPa was required to achieve 100% liquid fraction and 90 min from bonding time. Vice versa, for the 60% liquid fraction and bonding time at 45 min, the minimum bond strength was only 3.01 MPa because the high solids proportion of the atoms on the solder material were difficult to diffuse and significantly caused the establishment of elongated voids. This liquid state allows atoms to diffuse more freedom. Observably, an increase in fraction tends increased bond strength. By considering from the 90% liquid fraction and both bonding time, the bond strength increase to 12.44 and 25.98 MPa. The results of this study clearly show that liquid fraction influence the changes of bond strength and found to be related to bonding time significantly. Notwithstanding, the enlargement, swelling and buckling are plastic deformations that negatively affect the bond strength [17].

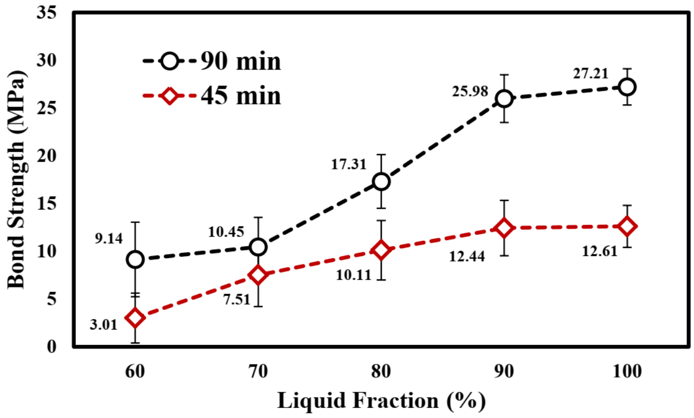

Figure 3. Bond strength comparison of TLP diffusion bonding samples according to the liquid fraction with bonding time.

Zn Atoms Diffused Distance along the Bond Line. The liquid fraction has a lot of influence on the motion dynamic freedom of atoms. In this research, the focus was to study the distance of Zn atomic diffusion due to the MgZn2 intermetallic compound formation. Therefore, this study used Scanning Electron Microscope (SEM) with Energy Dispersive X-Ray Spectrometer (EDS) mode to analyze the distribution and distance of elements which can be diffused farthest. The liquid fraction ratio affects the activation energy of atomic motion [18], in which the liquid fraction was at 100% value found that Zn atoms have the ability to move about 4.381 and 4.016 mm for 90 and 45 min of bonding time. The freedom of movement of atoms affects the elimination of gaps in the bond line and leads to the perfection of the workpiece. On the other hand, the Zn atoms have a low ability to diffuse in the solid state, which can be considered from 60% liquid fraction of the entire bonding time showing that the diffusion distance were at 2.023 and 2.219 mm respectively. The liquid fraction and bonding time are related to the diffusion distance of Zn atoms in ZA27 zinc alloy shown in Table 3.

Table 3. The distance of Zn atom diffused from EDX analyzed.

Liquid Fraction (%)	EDS analysis (mm)	
	45 min	90 min
60	2.023	2.219
70	3.014	3.307
80	3.299	3.750
90	3.718	4.248
100	4.016	4.381

Microstructural Changes Analysis. The optimized workpieces from the 100% liquid fraction and bonding time at 90 min were presented to characterize the microstructures that resulted in changes in the bond line shown in Fig. 4. In the macro photography, the deflection of the workpiece is shown in (Fig. 4(a)). Meanwhile, the microphotography demonstrates the obvious borderline of ZA27 zinc alloy, but notice that the borderline was a completed bond line which is a homogeneous joint. However, grains' globular morphology is related to heat resulting an enlarged appearance and loss of nodularity [19] (Fig. 4(b)). The gap between the solder material with the substrate material is completely eliminated (Fig. 4(c)). When analyze with color mapping mode in EDS, the uniform distribution of the elements was observed (Fig. 4(d)). When specifying the difference in the distribution of the elements, Zn elements are isostatic diffused. The distribution of Zn elements precipitated with other elements leading to the formation of $MgZn_2$ and $CuZn_4$ intermetallic compounds and encouraged to an increased hardness [20] (Fig. 5(e)). For quantitative analysis, Al elements were generally found with a high quantity at 52.21%wt, the Zn elements were at 13.49%wt and finally the Si elements were at 9.44%wt. These elements are important for the formation of intermetallic compounds (Fig. 5(f and g)).

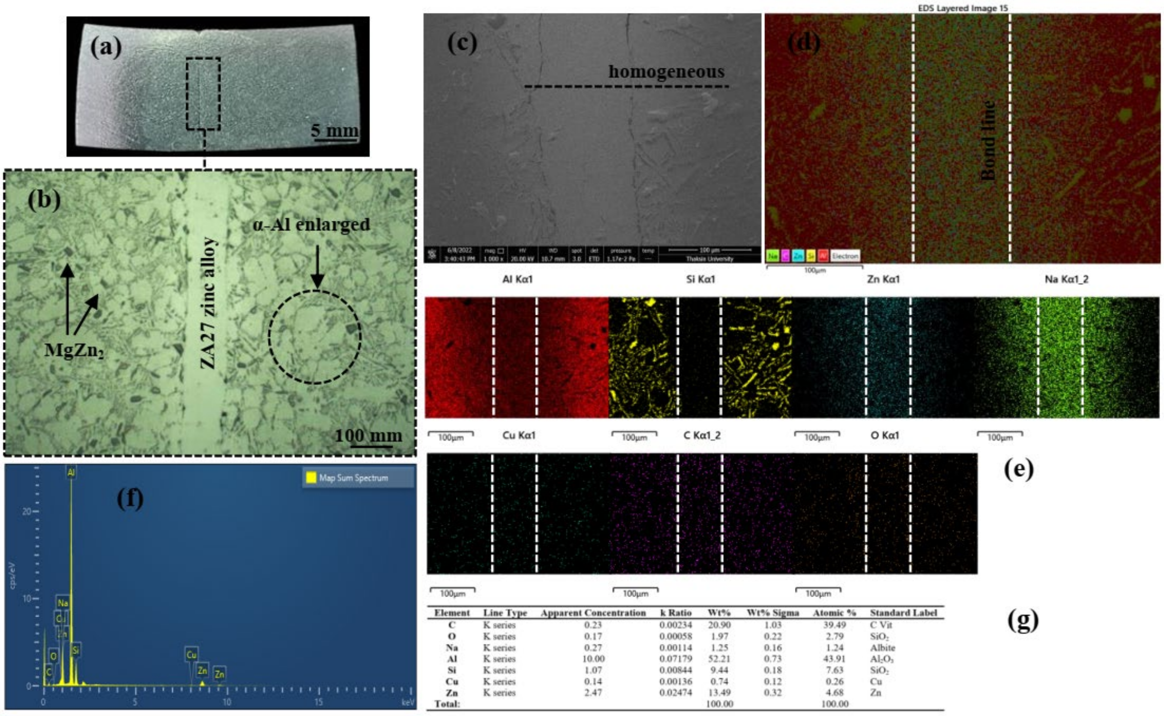

Element	Line Type	Apparent Concentration	k Ratio	Wt%	Wt% Sigma	Atomic %	Standard Label
C	K series	0.23	0.00234	20.90	1.03	39.49	C Vit
O	K series	0.17	0.00058	1.97	0.22	2.79	SiO_2
Na	K series	0.27	0.00114	1.25	0.16	1.24	Albite
Al	K series	10.00	0.07179	52.21	0.73	43.91	Al_2O_3
Si	K series	1.07	0.00844	9.44	0.18	7.63	SiO_2
Cu	K series	0.14	0.00136	0.74	0.12	0.26	Cu
Zn	K series	2.47	0.02474	13.49	0.32	4.68	Zn
Total:				100.00		100.00	

Figure 4. Macro and microstructural analysis defects, microstructural changes and elements distribution from TLP diffusion bonding: (a-b) Optical micrographs, (c) SEM micrographs and (d-g) EDS micrographs.

Hardness Analysis. Fig. 5 shows the Vickers hardness profiles distribution along the cross-section of the bond line of 100% liquid fraction and 90 min from bonding time, in which the hardness increased from the base material because of the obvious thermal during TLP diffusion bonding. Noteworthy, the maximum hardness zones located at the bond line because the $MgZn_2$ and $CuZn_4$ intermetallic compound was formatted and stress concentration caused by the accumulation of pressure [20]. The hardness values ranging from 121-119 HV and the value increase approximately 23.36% for the SSC-ADC12 aluminum alloy and 11.18% for ZA27 zinc alloy when the base hardness of SSC-ADC12 aluminum alloy was at 92.50 HV and 107.20 HV respectively. However, the hardness decreased in the local area next to the bond line because Zn atoms were unable to diffuse resulting incomplete formation of $MgZn_2$ and $CuZn_4$ intermetallic compounds [21]. This zone also found intermetallic compound formation in the form of $CuZn_4$ phase and hardness values ranging from 118-117 HV were investigated. In the zone near the end of the workpiece, the hardness values range from 114-116 HV where hardness increased slightly ascribable intermetallic compound still forming in its original state. In this phase, it is also regarded as Mg_2Si phase but precipitated at the grain boundary causing an increased hardness.

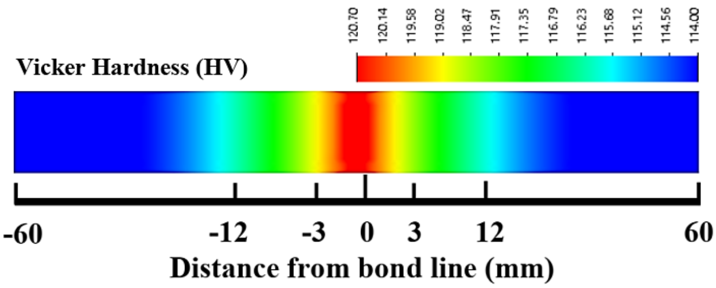

Figure 5. Vickers hardness profiles distribution in the cross-section of the welds.

Conclusion

The liquid fraction of ZA27 zinc alloy interlayer with SSC-ADC12 aluminum alloy workpieces during TLP diffusion bonding could affect characterizations of the workpiece, bond strength, hardness and microstructural changes in the bond line. In relatively high liquid fraction, enlargement, swelling and buckling were observed. The bond strength results were in good agreement with the 100% liquid fraction and 90 min bonding time which offered the maximum bond strength for 27.21 MPa. On the contrary, the minimum bond strength at 3.01 MPa was from 60% liquid fraction with the bonding time at 45 min. The hardness was increased by approximately 23.36% and 11.18% from SSC-ADC12 aluminum alloy and ZA27 zinc alloy respectively. The maximum hardness values ranged from 121-119 HV in the bond line due to the $MgZn_2$ intermetallic compound. Finally, the EDS analysis found that the maximum Zn atom diffusion distance was 4.381 mm from 100% liquid fraction and 90 min from bonding time. In the bond line, $MgZn_2$ and $CuZn_4$ intermetallic compound was formed and the Zn elements were in good move with the color mapping EDS estimated results.

Acknowledgements

This study was supported by the Faculty of Industrial Technology, Songkhla Rajabhat University (Thailand). We have got many supported apparatus from the Production Engineering of the Rajamangala University of Technology Srivijaya, Songkhla in Thailand.

References

[1] R. Bakhtiari, A. Ekrami, Mater. Des. 40 (2012) p. 130-137.

[2] A. AlHazaa, T.I. Khan, I. Haq, Mater. Charact. 61 (2010) p. 312-317.

[3] Anas M. Atieh, Marcelo Epstein, Mater. Today Commun. 25 (2020) 101481.

[4] C. Meengam, Y. Dunyakul, D. Maunkhaw, S. Chainarong, Metals. 8 (2018) p. 1-13.

[5] E. Lugscheider, K. Bobzin, A. Erdle, Surf. Coat. Technol. 174-175 (2003) p. 704-707.

[6] Mohammad Ali Karimi, Morteza Shamanian, Mohammad Hossein Enayati, Trans. Nonferrous Met. Soc. China. 31(10) (2021) p. 3063-3074.

[7] Lin Yuan, Jiangtao Xiong, Jin Ren, Yajie Du, Jinglong Li, Mater. Charact. 178 (2021) 111292.

[8] M. Soltani Samani, A. Bahrami, F. Karimzadeh, Mater. Today Commun. 21 (2019) 100619.

[9] A. Malekan, S.E. Mirsalehi, M. Farvizi, N. Saito, K. Nakashima, Trans. Nonferrous Met. Soc. China. 32(5) (2022) p. 1548-1558.

[10] Zhiyu Chang, Xingchen Wang, Yujuan Wu, Liming Peng, Wenjiang Ding, Mater. Lett. 282 (2021) 128835.

[11] Wenying Qu, Juan Chen, Zhong Li, Min Luo, Hongxing Lu, Xiaogang Hu, Qiang Zhu, Mater. Lett. 220 (2022) 114932.

[12] Suppachai Chainarong, Rapeepan Pitakaso, Worapot Sirirak, Thanatkij Srichok, Surajet Khonjun, Kanchana Sethanan, Thai Sangthean, J. Manuf. Mater. Process. 5(4) (2021) 123.

[13] Nai-yong LI, Wei-min Mao, Xiao-xin Geng, Trans. Nonferrous Met. Soc. China. 32(3) (2022) p. 739-749.

[14] J. Wannasin, R. Canyook, S. Wisutmethangoon, M.C. Flemings, Acta Mater. 61 (2013) p. 3897-3903.

[15] Hengyu Zhao, Satoshi Uda, Kensaku Maeda, Jun Nozawa, Haruhiko Koizumi, Kozo Fujiwara, J. Cryst. Growth. 415 (2015) p. 111-117.

[16] Hongqiang Zhang, Junliang Xue, Yu Ye, Hailin Bai, Wei Guo, Guisheng Zou, Lei Liu, J. Alloys Compd. 909 (2022) 164692.

[17] Song-Mao Liang, Rainer Schmid-Fetzer, Calphad: Comput. Coupling Ph. Diagr. Thermochem. 52 (2016) p. 21-37.

[18] H. Nami, A. Halvaee, H. Adgi, Mater. Des. 32 (2011) p. 3957-3965.

[19] M. Mazar Atabaki, J. Idris, Mater. Des. 34 (2012) p. 832-841.

[20] Y.J. Jin, T.I. Khan, Mater. Des. 38 (2012) p. 32-37.

[21] M.S. Kenevisi, S.M. Mousavi Khoie, Mater. Des. 38 (2012) p. 19-25.